

Quantum simulation of Burgers turbulence: Nonlinear transformation and direct evaluation of statistical quantities

Fumio Uchida,^{1,*} Koichi Miyamoto,^{2,†} Soichiro Yamazaki,^{3,‡} Kotaro Fujisawa,^{4,5,§} and Naoki Yoshida^{3,6,¶}

¹*Theory Center, Institute of Particle and Nuclear Studies (IPNS),*

High Energy Accelerator Research Organization (KEK), Tsukuba, Ibaraki 305-0801, Japan

²*Center for Quantum Information and Quantum Biology,*

Osaka University, Toyonaka, Osaka 560-0043, Japan

³*Department of Physics, University of Tokyo, 7-3-1 Hongo, Bunkyo, Tokyo 113-0033, Japan*

⁴*Department of Liberal Arts, Tokyo University of Technology,*

5-23-22 Nishikamata, Ota, Tokyo, 144-8535, Japan

⁵*Research Center for the Early Universe (RESCEU), 7-3-1 Hongo, Bunkyo, Tokyo, 113-0033, Japan*

⁶*Kavli IPMU, WPI, University of Tokyo, 5-1-5 Kashiwanoha, Kashiwa, Chiba 277-8583, Japan*

(Dated: December 24, 2024)

Fault-tolerant quantum computing is a promising technology to solve linear partial differential equations that are classically demanding to integrate. It is still challenging to solve non-linear equations in fluid dynamics, such as the Burgers equation, using quantum computers. We propose a novel quantum algorithm to solve the Burgers equation. With the Cole–Hopf transformation that maps the fluid velocity field u to a new field ψ , we apply a sequence of quantum gates to solve the resulting linear equation and obtain the quantum state $|\psi\rangle$ that encodes the solution ψ . We also propose an efficient way to extract stochastic properties of u , namely the multi-point functions of u , from the quantum state of $|\psi\rangle$. Our algorithm offers an exponential advantage over the classical finite difference method in terms of the number of spatial grids when a perturbativity condition in the information-extracting step is met.

I. INTRODUCTION

With the recent rapid development of hardware platforms, quantum computing attracts great interest and hope in physical science [1–8], including cosmology and astrophysics [9–16]. Although we are still in the era of noisy intermediate-scale quantum technologies (NISQ) [17], there have been a variety of studies aimed at fault-tolerant quantum computing (FTQC) [18–21], which enables us to tackle classically intractable problems. Fluid dynamics continues to provide such challenging problems. For instance, [14–16, 22] proposed quantum algorithms to integrate the collisionless Boltzmann equation (CBE) [23], which describes the evolution of a dilute system such as rarefied gas, and cosmic neutrinos and dark matter in the structure formation of the universe.

There remains an “apparent” limitation that quantum computing is applicable to only linear problems in a direct manner because of the linearity of quantum operations. Although quantum algorithms to solve a wide class of linear problems have been proposed [24–29], solving nonlinear problems has been a challenging task for FTQC algorithms.

Nevertheless, applying quantum computing to non-linear problems such as the Navier–Stokes equation (NSE) is important and timely. The NSE is a nonlinear

partial differential equation that governs fluid dynamics [30], and there are a broad range of potential applications in astrophysics and cosmology, *e.g.* the primordial gravitational wave [31–33] and the primordial magnetic field [34–38] coupled with a photon-baryon plasma in the early universe, as listed in Ref. [39]. Although no general framework is known to efficiently solve the NSE, a variety of attempts have been proposed [40–45].

Several approaches have been proposed to deal with non-linear problems with FTQC algorithms. Many of them are based on linearization of the non-linear equations by introducing a large number of auxiliary variables [46–48]. Practically, we need to truncate auxiliary variables at a finite number, and this is guaranteed to work only for problems and systems with moderate non-linearity.

An intriguing example is the one-dimensional Burgers equation [49, 50]. It is a non-linear equation that describes the time evolution of fluid velocity u , and can be viewed as the simplest model of non-linear fluid dynamics and hence as an important first step to solve the full NSE [51, 52]. A crucial point is that the one-dimensional Burgers equation is transformed to a linear heat equation by the Cole–Hopf transformation [53, 54], which maps u to a new field ψ . However, this does not mean that Burgers turbulence is completely understood. Turbulence velocities are described by the Burgers equation, and its stochastic properties have been extensively investigated [55–60].

In the present study, we propose a quantum algorithm to measure the statistical properties of the one-dimensional Burgers turbulence. We apply the quantum differential equation solver [61] to the equation obtained

* fuchida@post.kek.jp

† miyamoto.kouichi.qiqb@osaka-u.ac.jp

‡ soichiro.yamazaki@phys.s.u-tokyo.ac.jp

§ kotaro.fujisawa@gmail.com

¶ naoki.yoshida@ipmu.jp

by the Cole–Hopf transformation on the Burgers equation to get the quantum state $|\psi\rangle$ that encodes the solution ψ in the amplitudes. Furthermore, from $|\psi\rangle$, we extract the statistical properties of the solution, specifically, the multi-point functions of u , via estimating expectation values of some operators. This is a well-defined and well-suited task for quantum computing. If one would like to understand the full real-space configuration, measurement with a given accuracy would cost an enormous time complexity. In contrast, we aim at deriving only a limited number of values as classical data from a quantum state, taking full advantage of a quantum speedup. In this information extraction step, due to the nonlinearity of the Cole–Hopf transformation, we need to apply a certain approximation that a perturbative nature holds with respect to ψ , which is non-trivial for fluid with a large Reynolds number. Nevertheless, when the perturbative condition holds, our algorithm offers an exponential advantage over the classical finite difference method in terms of the number of spatial grids. To validate our approach, we perform simple test calculations and show that the solution by our method is sufficiently accurate compared to that without the approximation.

The paper is organized as follows. In Sec. II, we introduce the Burgers equation and multi-point functions of the velocity field. In Sec. III, we present our algorithm to solve the Burgers equation and extract the multi-point functions from the solution-encoding quantum state. In Sec. IV, we discuss the complexity analysis for our algorithm and possible generalizations, along with presenting the results of numerical demonstrations. Sec. V concludes this paper.

II. BURGERS TURBULENCE

A. Burgers equation and Cole–Hopf transformation

We consider a velocity field $u(t, x)$ in one-dimensional system, which is governed by the Burgers equation

$$\partial_t u + u \partial_x u = \nu \partial_x^2 u, \quad (1)$$

where $\nu > 0$ is a viscosity coefficient that dissipates kinetic energy into heat. The advection term introduces a nonlinearity, of which significance may be quantified as the Reynolds number,

$$\text{Re} := \frac{ul}{\nu}, \quad (2)$$

where l is the typical length scale of the system, and $\text{Re} \gg 1$ implies a highly nonlinear state.

However, irrespectively of how large the Reynolds number is, Hopf [53] and Cole [54] found that, by introducing a new field ψ , *s.t.*

$$\psi = \exp\left(-\frac{1}{2\nu} \int^x dy u(y)\right), \quad (3)$$

or equivalently,

$$u = -2\nu \frac{\partial_x \psi}{\psi}, \quad (4)$$

Eq. (1) is reduced to a linear heat equation

$$\partial_t \psi = \nu \partial_x^2 \psi. \quad (5)$$

The heat equation can be formally integrated, although its numerical evaluation is not necessarily easy. Our aim is to bypass the *nonlinearity* of the original problem with the Cole–Hopf transformation and take advantage of the *linear* nature of quantum computing. Note that solving the heat equation with a quantum speedup is an area of study [62], but we do not extensively investigate this point in this work.

B. Statistical quantities of Burgers turbulence

We suppose that we are interested in statistical quantities, namely the multi-point functions, of the velocity field. We define the multi-point functions $P^{(n)}$ and the higher-order moments $I^{(n)}$ for $n \geq 2$ of the velocity field

$$P^{(n)}(\{x_i - x_0\}_{i=1, \dots, n-1}, t) := \overline{\prod_{i=0}^{n-1} u(x_i, t)}, \quad (6)$$

$$I^{(n)}(t) := P^{(n)}(\{0\}_{i=0, \dots, n-1}, t), \quad (7)$$

where the bar takes a volume average, where $\overline{X(\{x_i\}_i)} := (1/L) \int_0^L dx' X(\{x' + x_i\}_i)$ for a general function X with the periodic boundary condition, of the inside. We may further average over ensembles, when we have a bunch of random initial conditions, to explore the universal properties of turbulence with those initial conditions.

In the following sections, we will propose an algorithm to measure these quantities up to a common normalization factor among all the quantities.

III. QUANTUM ALGORITHM

In this section, we will explain that the Burgers equation can be solved efficiently, by using a quantum computer.

The algorithm to compute the multi-point functions for one realization of the velocity field proceeds in the following three steps:

- Classical to quantum:
loading the initial condition into the quantum state (Sec. III A)
- Quantum operation:
integration of the heat equation (Sec. III B)
- Quantum to classical:
extracting the wanted information (Sec. III C)

On top of this, in Sec. III D, we explain how to efficiently take an ensemble average of the multi-point functions.

A. Implementing the initial condition

We discretize the spatial coordinate $0 \leq x \leq L$ into $N_x = 2^{n_x}$ grids and impose, for now, the periodic boundary condition. Generalization to non-periodic conditions will be discussed in Sec. IV. We assume that we have an oracle $O_{\psi'_0}$ to generate a quantum state encoding the initial value of $\partial_x \psi$:

$$O_{\psi'_0} |\mathbf{0}\rangle = |\partial_x \psi(0)\rangle. \quad (8)$$

Here, we define

$$|\partial_x \psi(t)\rangle := \sum_{j=0}^{N_x-1} \frac{\partial_x \psi_j(t)}{\mathcal{N}(t)} |j\rangle \quad (9)$$

where $\partial_x \psi_j(t) := \partial_x \psi(j\Delta x, t)$, and $\Delta x := L/N_x$. A normalization factor \mathcal{N} is introduced so that $\langle \partial_x \psi(t) | \partial_x \psi(t) \rangle = 1$.

The methods to generate a quantum state encoding a known function like Eq. (9) have been investigated in the literature. For example, if $\partial_x \psi(x, 0)$ is analytically calculated and satisfies some conditions, the Grover-Rudolph method [63] and other methods [64–68] can be used. If $\partial_x \psi_j(0)$ is given pointwise and the values are stored in the quantum random access memory [69], we can generate $|\partial_x \psi(0)\rangle$ by the method in Ref. [70].

B. Integration of the heat equation

Let us discretize the heat equation (5). In terms of $\partial_x \psi$, Eq. (5) is

$$\partial_t \partial_x \psi = \nu \partial_x^2 \partial_x \psi. \quad (10)$$

By normalizing the temporal coordinate properly and discretizing the spatial coordinate, it becomes

$$\frac{d\partial_x \psi_j}{d\tau} = \partial_x \psi_{j-1} - 2\partial_x \psi_j + \partial_x \psi_{j+1}, \quad j \in \mathbb{Z}_{N_x}, \quad (11)$$

where we introduced a normalized temporal coordinate $\tau := \nu t / \Delta x^2$. Equation (11) can also be written as

$$\frac{d\partial_x \psi}{d\tau} = A \partial_x \psi, \quad A := \begin{pmatrix} -2 & 1 & 0 & \cdots & 1 \\ 1 & -2 & 1 & \cdots & 0 \\ 0 & 1 & -2 & \cdots & 0 \\ & & \cdots & & \\ 1 & 0 & \cdots & 1 & -2 \end{pmatrix}, \quad (12)$$

which is integrated formally as

$$\partial_x \psi(\tau) = e^{A\tau} \partial_x \psi(0). \quad (13)$$

Obtaining $|\partial_x \psi(\tau)\rangle$ as a quantum state is possible as shown in Corollary 16 of Ref. [61]. By noting $\|A\| \leq$

$\sqrt{\|A\|_1 \|A\|_\infty} = 4^1$, an oracle $O_{\psi'_\tau}$ that act on the initial state $|\partial_x \psi(0)\rangle$ to generate $|\partial_x \psi(\tau)\rangle$ with an error tolerance $\epsilon_1 > 0$ costs

$$\tilde{\mathcal{O}} \left(\frac{\|\partial_x \psi_0\|}{\|\partial_x \psi(\tau)\|} \tau \times \text{polylog} \left(\frac{1}{\epsilon_1} \right) \right) \text{ queries to } U_A, \quad (14)$$

$$\text{and } \mathcal{O} \left(\frac{\|\partial_x \psi_0\|}{\|\partial_x \psi(\tau)\|} \right) \text{ queries to } O_{\psi'_0}, \quad (15)$$

where U_A is a block-encoding of A . If the block-encoding of A has an error ϵ_2 , the factor $e^{A\tau}$ in Eq. (13) has a relative error $\epsilon_2 \tau$, resulting in a total error $\epsilon_1 + \epsilon_2 \tau$ for the state $|\partial_x \psi(\tau)\rangle$. According to Ref. [71] (Lemma 48 in the full-version), with A 's sparsity and max norm being 3 and 2, respectively, we can implement a $(6, n_x + 3, \epsilon_2)$ block-encoding² of A , using

$$\mathcal{O} \left(n_x + \log^{\frac{5}{2}} \left(\frac{18}{\epsilon_2} \right) \right) \text{ fundamental gates} \quad (16)$$

and $\mathcal{O}(\log^{5/2}(18/\epsilon_2))$ ancilla qubits, along with

$$\mathcal{O}(1) \text{ calls to the sparse-access oracles for } A. \quad (17)$$

We will discuss query complexity of our algorithm in terms of the numbers of uses of the sparse-access oracles, which access elements of a sparse matrix, and fundamental gates, *i.e.*, a universal set of one- and two-qubit gates, not included therein.

At this point, we have an oracle $O_{\psi'_\tau} O_{\psi'_0}$ to generate the “solution” state $|\partial_x \psi(\tau)\rangle$, which has values of $\partial_x \psi_j(\tau)$ in the amplitude of $|j\rangle$. Nonlinearity in terms of u and high spatial resolution is achieved up to limitations originating from the finite discretization scheme.

However, extracting arbitrary information from a quantum state is a non-trivial task, and we address this issue in the next section.

C. Retrieving the desired information

In this step, we introduce approximations to extract statistical information on the velocity field u . We begin by discussing the two- and three-point functions $P^{(2)}$ and $P^{(3)}$, and then generalize them to higher-order multi-point functions.

1. Two-point function

We apply a perturbative description to linearize the relation between ψ and u . We approximate the velocity field

¹ For $M = (m_{ij}) \in \mathbb{C}^{m \times n}$, $\|M\|$ denotes its spectral norm, $\|M\|_1 = \max_j \sum_{i=1}^m |m_{ij}|$, and $\|M\|_\infty = \max_i \sum_{j=1}^n |m_{ij}|$.

² For the definition of (α, a, ϵ) block-encoding, where $\alpha, \epsilon > 0$ and $a \in \mathbb{N}$, see Ref. [71].

u as

$$u_j \simeq -\frac{\nu \partial_x \psi_j}{\bar{\psi}}, \quad (18)$$

where we replace ψ in the denominator with the spatial average $\bar{\psi} := \frac{1}{L} \int_0^L \psi(x, t) dx$. Hereafter, we will consider the statistics on the right-hand side of Eq. (18), but identifying both sides is not always trivial. See the discussion in Sec. IV. With this approximation, we have

$$\begin{aligned} |\mathbf{u}\rangle &:= \sum_j \frac{u_j}{\|\mathbf{u}\|} |j\rangle \\ &\simeq -|\partial_x \psi(t)\rangle. \end{aligned} \quad (19)$$

Then, the two-point function of the velocity field $P^{(2)}(r = \rho \Delta x)$, $\rho \in \mathbb{Z}_{N_x}$ can be approximated as

$$\begin{aligned} P^{(2)}(r) &= \overline{u(x)u(x+r)} \\ &= N_x^{-1} \sum_{k=0}^{N_x-1} u_k u_{k+\rho} \\ &= N_x^{-1} \|\mathbf{u}\|^2 \sum_{j,k=0}^{N_x-1} C_{jk}^{(2)}(\rho) \frac{u_j}{\|\mathbf{u}\|} \frac{u_k}{\|\mathbf{u}\|}. \end{aligned} \quad (20)$$

Here, $C_{jk}^{(2)}(\rho)$ is given by

$$C_{jk}^{(2)}(\rho) := \sum_{\sigma, \sigma'} \delta_{j-\sigma, k-\sigma'} c_{\sigma\sigma'}^{(2)}(\rho), \quad (21)$$

where

$$c_{\sigma\sigma'}^{(2)}(\rho) := \begin{cases} +\frac{1}{2} & (\sigma, \sigma') = (0, \rho), \\ +\frac{1}{2} & (\sigma, \sigma') = (\rho, 0), \\ 0 & \text{otherwise} \end{cases} \quad (22)$$

for $\rho \neq 0$, and

$$c_{\sigma\sigma'}^{(2)}(0) := \begin{cases} 1 & \sigma = \sigma' = 0, \\ 0 & \text{otherwise} \end{cases} \quad (23)$$

for $\rho = 0$. From Eq. (20), we obtain an expression for the two-point function $P^{(2)}(r, \tau)$ normalized by the second moment $I^{(2)}(\tau) = P^{(2)}(0, \tau)$,

$$\frac{P^{(2)}(r, \tau)}{I^{(2)}(\tau)} = \frac{\langle \mathbf{u}(\tau) | C^{(2)}(\rho) | \mathbf{u}(\tau) \rangle}{\langle \mathbf{u}(\tau) | C^{(2)}(0) | \mathbf{u}(\tau) \rangle}. \quad (24)$$

Both the numerator and the denominator are $\mathcal{O}(1)$ quantities, as understood from the expression in Eq. (20), where $N_x^{-1} \|\mathbf{u}\|^2 = \mathcal{O}(1)$.

The values of the numerator and the denominator in the right-hand side can be measured by applying the overlap estimation algorithm [72]. For that purpose, we decompose $C^{(2)}(\rho)$ as

$$C^{(2)}(\rho) = \frac{1}{2} (P_{N_x}^\rho + P_{N_x}^{-\rho}), \quad (25)$$

where P_{N_x} is the cyclic increment

$$P_{N_x} := \sum_{j=0}^{N_x-2} |j+1\rangle \langle j| + |0\rangle \langle N_x-1|, \quad (26)$$

which is implemented with $\mathcal{O}(n_x)$ fundamental gates and ancilla qubits [73]. Therefore, for $\rho = \sum_{a=0}^{n_x} \rho_a 2^a$, because we can decompose $P_{N_x}^\rho$ as $P_{N_x}^\rho = \prod_{a=0}^{n_x} \delta_{\rho_a, 1} P_{2^{n_x-a}} \otimes 1_{2^a}$, we can construct $P_{N_x}^\rho$ with

$$\mathcal{O}(n_x^2) \text{ fundamental gates} \quad (27)$$

and $\mathcal{O}(n_x)$ ancilla qubits, which is reused in each $P_{2^{n_x-a}}$.

Since $P_{N_x}^\rho$ is unitary, we can estimate $\langle \mathbf{u}(\tau) | P_{N_x}^\rho | \mathbf{u}(\tau) \rangle$ by the overlap estimation algorithm in [72], making

$$\mathcal{O}\left(\frac{1}{\epsilon_3}\right) \text{ queries to } P_{N_x}^{\pm\rho}, P_{N_x}^{\pm\rho \pm 2}, \text{ and } O_{u_\tau}, \quad (28)$$

where $O_{u_\tau} := -O_{\psi'_\tau} O_{\psi'_0}$, to achieve an error tolerance $\epsilon_3 > 0$. After measuring the numerator and the denominator separately, one can obtain the value of Eq. (24) for given r and τ with the precision $\epsilon_1 + \tau\epsilon_2 + \epsilon_3$.

2. Three-point function

Next, we discuss the three-point functions of the velocity field. To reduce the computational complexity of reading out classical information, we introduce sub-grids, $x_{\text{c}gk} := 2^{n_x-m} k \Delta x$, where an integer $m \geq 1$ is taken independent of n_x , and coarse-grain the high-resolution $|\mathbf{u}\rangle$ onto the sub-grids. This is motivated when the small-scale modes are nonsignificant because increasing n_x beyond the smallest among the relevant scales of turbulence would not provide better information. We can integrate out the small-scale modes within each sub-grid by acting Hadamard gates on the subspace corresponding to the last $n_x - m$ digits of each $|j\rangle$:

$$\begin{aligned} |\mathbf{u}\rangle_{\text{cg}} &:= 1_{2^m} \otimes H^{\otimes n_x-m} |\mathbf{u}\rangle \\ &= \sum_{k=0}^{2^m-1} u_{\text{c}gk} |k\rangle_{\text{ss}} + |\perp\rangle, \end{aligned} \quad (29)$$

where H is the Hadamard gate,

$$u_{\text{c}gk} := 2^{-\frac{n_x-m}{2}} \sum_{j=2^{n_x-m}k}^{2^{n_x-m}(k+1)-1} \frac{u_j}{\|\mathbf{u}\|}, \quad (30)$$

$|0\rangle_{\text{ss}} := |0\rangle^{\otimes n_x-m}$, 1_{2^m} is the identity operator on the first m qubits, and $|\perp\rangle$ is a garbage state such that $(1_{2^m} \otimes |0\rangle_{\text{ss}} \langle 0|_{\text{ss}}) |\perp\rangle = 0$. Hereafter, we define $O_{u_{\text{cg}}} := (1_{2^m} \otimes H^{\otimes n_x-m}) O_{u_\tau}$ so that $O_{u_{\text{cg}}} |\mathbf{0}\rangle = |\mathbf{u}\rangle_{\text{cg}}$.

Then, a three-point function of the velocity field $P^{(3)}(r_1 = 2^{n_x-m} \rho_1 \Delta x, r_2 = 2^{n_x-m} \rho_2 \Delta x)$, $\rho_1, \rho_2 \in \mathbb{Z}_{2^m}$ can be approximated as

$$P^{(3)}(r_1, r_2)$$

$$\begin{aligned}
&\simeq 2^{-n_x} \sum_{j=0}^{2^{n_x}-1} u_j u_{j+2^{n_x-m}\rho_1} u_{j+2^{n_x-m}\rho_2} \\
&\simeq 2^{-\frac{3}{2}n_x + \frac{1}{2}m} \|\mathbf{u}\|^3 \sum_{j,k,l=0}^{2^m-1} C_{jkl}^{(3)}(\rho_1, \rho_2) u_{\text{cg } j} u_{\text{cg } k} u_{\text{cg } l}. \quad (31)
\end{aligned}$$

Here, in the second equality, we replace u_j , $j \in [2^{n_x-m}k, 2^{n_x-m}(k+1) - 1]$ with

$$2^{-(n_x-m)} \sum_{j'=2^{n_x-m}k}^{2^{n_x-m}(k+1)-1} u_{j'} = 2^{-\frac{n_x-m}{2}} \|\mathbf{u}\| u_{\text{cg } k}, \quad (32)$$

assuming that u is coherent over the length scale $2^{-m}L$, *i.e.*, smaller-scale modes within the scale $2^{-m}L$ are subdominant. We define

$$C_{jkl}^{(3)}(\rho_1, \rho_2) := \sum_{\sigma, \sigma', \sigma''} \delta_{j-\sigma, k-\sigma'} \delta_{j-\sigma, l-\sigma''} c_{\sigma\sigma'\sigma''}^{(3)}(\rho_1, \rho_2) \quad (33)$$

and

$$c_{\sigma\sigma'\sigma''}^{(3)}(\rho_1, \rho_2) := \mathcal{S} \left[\begin{cases} 1 & (\sigma, \sigma', \sigma'') = (0, \rho_1, \rho_2) \\ 0 & \text{otherwise} \end{cases} \right], \quad (34)$$

where \mathcal{S} is symmetrization with respect to the indices. Note that the prefactor in front of the summation in Eq. (31) scales as $\mathcal{O}(2^{m/2})$, independently of n_x .

From Eq. (31), we obtain an expression for the three-point function $P^{(3)}(r_1, r_2, \tau)$ normalized by the third moment $I^{(3)}(\tau) = P^{(3)}(0, 0, \tau)$,

$$\frac{P^{(3)}(r_1, r_2, \tau)}{I^{(3)}(\tau)} = \frac{\langle U^{(3)}(\tau) | \tilde{C}^{(3)}(\rho_1, \rho_2) | U^{(3)}(\tau) \rangle}{\langle U^{(3)}(\tau) | \tilde{C}^{(3)}(0, 0) | U^{(3)}(\tau) \rangle}, \quad (35)$$

where we define

$$\begin{aligned}
|U^{(3)}\rangle &:= \frac{|\mathbf{u}\rangle_{\text{cg}}^{\otimes 2} \otimes |0\rangle + |\mathbf{u}\rangle_{\text{cg}} \otimes |\mathbf{0}\rangle \otimes |1\rangle}{\sqrt{2}} \\
&= \sum_{j,k} \frac{u_{\text{cg } j} u_{\text{cg } k}}{\sqrt{2}} |j, k, 0\rangle + \sum_l \frac{u_{\text{cg } l}}{\sqrt{2}} |l, 0, 1\rangle + |\perp\rangle, \quad (36)
\end{aligned}$$

$$(37)$$

and

$$\begin{aligned}
\tilde{C}^{(3)} &:= \sum_{j,k,l=1}^{N_x} C_{jkl}^{(3)} \frac{|j, k, 0\rangle \langle l, 0, 1| + |l, 0, 1\rangle \langle j, k, 0|}{2} \\
&\quad \otimes |0\rangle_{\text{ss}} \langle 0|_{\text{ss}}, \quad (38)
\end{aligned}$$

where $|\perp\rangle$ is the garbage state originating from the one that $|\mathbf{u}\rangle_{\text{cg}}$ has, and the projection $|0\rangle_{\text{ss}} \langle 0|_{\text{ss}}$ eliminates the garbage state. Note that, since the prefactor in the last line in Eq. (31) scales as $2^{m/2}$, the numerator and the denominator in the right-hand side of Eq. (35) are $\mathcal{O}(2^{-m/2})$.

The state $|U^{(3)}\rangle = O_{U^{(3)}}|0\rangle$, where $O_{U^{(3)}} := O_{\text{cg}} \otimes [CO_{\text{cg}}(1_{N_x} \otimes H)]$, and H is the Hadamard gate, can be

constructed if we have $CO_{\text{cg}} := 1_{N_x} \otimes |0\rangle \langle 0| + O_{\text{cg}} \otimes |1\rangle \langle 1|$, namely a controlled- O_{cg} operation. In the complexity estimate, we assume that CO_{cg} requires the same query complexity as O_{cg} does.

The operator $\tilde{C}^{(3)}$ is a matrix of $\mathcal{O}(1)$ sparsity and maximum norm, and it has an $(\mathcal{O}(1), \mathcal{O}(n_x), \epsilon_4)$ block-encoding $\mathcal{C}^{(3)}$ with $\mathcal{O}(n_x)$ ancilla qubits. To construct this, we make $\mathcal{O}(1)$ queries to the sparse-access oracles for $\tilde{C}^{(3)}$ and use

$$\mathcal{O} \left(n_x + \log^{\frac{5}{2}} \left(\frac{1}{\epsilon_4} \right) \right) \text{ fundamental gates} \quad (39)$$

and $\mathcal{O}(\log^{5/2}(1/\epsilon_4))$ ancilla qubits [71].

Since $\mathcal{C}^{(3)}$ is unitary, the numerator and the denominator in the right-hand side of Eq. (35) can be measured with the error tolerance $2^{-m/2}\epsilon_3$ by the overlap estimation algorithm [72], which makes

$$\mathcal{O} \left(\frac{2^{\frac{m}{2}}}{\epsilon_3} \right) \text{ queries to } \mathcal{C}^{(3)} \text{ and } O_{U^{(3)}}. \quad (40)$$

Then, after measuring the numerator and the denominator separately, one may obtain the value of Eq. (35) for given r_1, r_2 , and t , with an error tolerance ϵ_3 . Note that, if one skips the coarse-graining procedure by taking $m = n_x$, we need $2^{-n_x/2}\epsilon_3$ accuracy in the overlap estimation algorithm to achieve an error tolerance ϵ_3 in evaluating Eq. (35), implying an exponentially larger query complexity in Eq. (40).

3. Higher-order multi-point function

We then generalize the procedure to the higher-order multi-point functions. For a general integer n , we may approximate

$$\begin{aligned}
P^{(n)}(\mathbf{r}) &= 2^{-\frac{n}{2}n_x + \frac{n-2}{2}m} \|\mathbf{u}\|^n \sum_j C_j^{(n)}(\boldsymbol{\rho}) \prod_{i=1}^n u_{\text{cg } j_i}, \quad (41)
\end{aligned}$$

where $\mathbf{r} = (r_1, \dots, r_{n-1})$, $r_0 = 0$, $\boldsymbol{\rho} = 2^{-n_x+m}\mathbf{r}/\Delta x \in \mathbb{Z}^{n-1}$, and $\mathbf{j} = (j_1, \dots, j_n)$, respectively. The matrix $C^{(n)}$ is defined such that

$$C_j^{(n)}(\boldsymbol{\rho}) := \sum_{\boldsymbol{\sigma}} \delta_{j-\boldsymbol{\sigma}} c_{\boldsymbol{\sigma}}^{(n)}(\boldsymbol{\rho}), \quad (42)$$

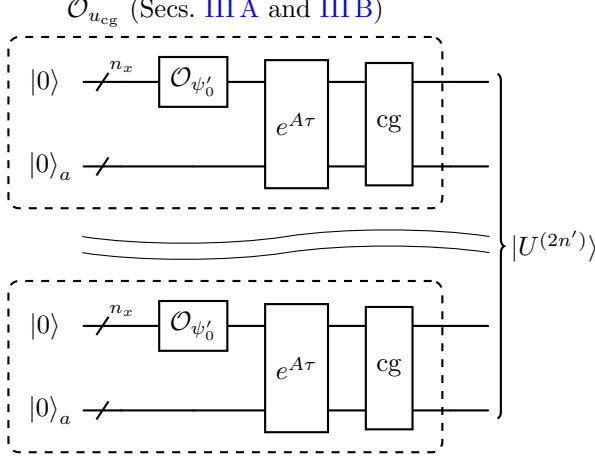
$$c_{\boldsymbol{\sigma}}^{(n)}(\boldsymbol{\rho}) := \mathcal{S} \left[\begin{cases} 1 & \boldsymbol{\sigma} = \boldsymbol{\rho} \\ 0 & \text{otherwise} \end{cases} \right], \quad (43)$$

where \mathcal{S} is symmetrization with respect to the indices σ_i .

If $n = 2n'$ is an even number, we define

$$|U^{(2n')}\rangle := O_{U^{(2n')}}|0\rangle = |\mathbf{u}\rangle_{\text{cg}}^{\otimes n'}, \quad (44)$$

where $O_{U^{(2n')}} := O_{\text{cg}}^{\otimes n'}$ is constructed by the following quantum circuit,



where cg denotes the coarse-graining procedure. We also define

$$\tilde{C}^{(2n')} := \sum_j C_j^{(2n')} \left(\frac{|j_1, \dots, j_{n'}\rangle \langle j_{n'+1}, \dots, j_{2n'}|}{2} + \frac{|j_{n'+1}, \dots, j_{2n'}\rangle \langle j_1, \dots, j_{n'}|}{2} \right). \quad (45)$$

This is $n!$ -sparse and has an $(\mathcal{O}(n!), \mathcal{O}(nn_x), \epsilon_4)$ block-encoding $\tilde{C}^{(n)}$, which is constructed with

$$\mathcal{O}(1) \text{ queries to the sparse-access oracles for } \tilde{C}^{(n)} \quad (46)$$

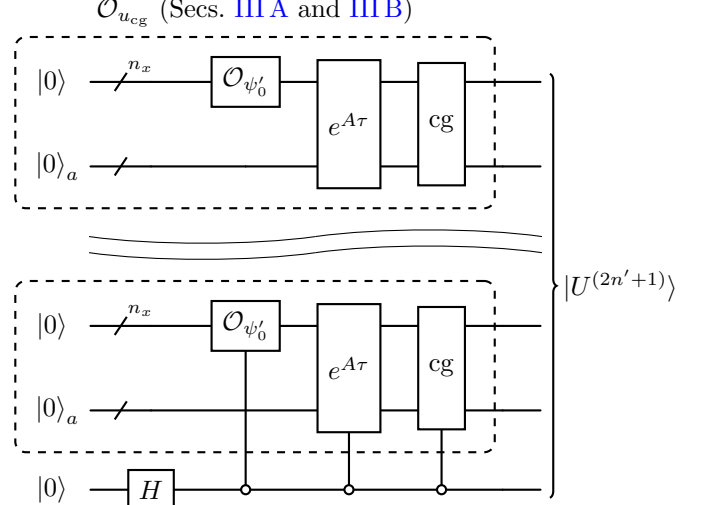
and

$$\mathcal{O} \left(nn_x + \log^{\frac{5}{2}} \left(\frac{n!}{\epsilon_4} \right) \right) \text{ fundamental gates.} \quad (47)$$

If $n = 2n' + 1$ is an odd number, we define

$$|U^{(2n'+1)}\rangle := O_{U^{(2n'+1)}} |0\rangle = \frac{|\mathbf{u}\rangle_{\text{cg}}^{\otimes n'+1} \otimes |0\rangle + |\mathbf{u}\rangle_{\text{cg}}^{\otimes n'} \otimes |\mathbf{0}\rangle \otimes |1\rangle}{\sqrt{2}}, \quad (48)$$

where $O_{U^{(2n'+1)}} := O_{\text{u}_{\text{cg}}}^{\otimes n'} \otimes [CO_{\text{u}_{\text{cg}}}(1_{N_x} \otimes H)]$ is constructed by the following quantum circuit,



and

$$\tilde{C}^{(2m+1)} := \sum_j C_j^{(2n'+1)} \left(\frac{|j_1, \dots, j_{n'+1}, 0\rangle \langle j_{n'+2}, \dots, j_{2n'+1}, 0, 1|}{2} + \frac{|j_{n'+2}, \dots, j_{2n'+1}, 0, 1\rangle \langle j_1, \dots, j_{n'+1}, 0|}{2} \right), \quad (49)$$

which also has an $(\mathcal{O}(n!), \mathcal{O}(nn_x), \epsilon_4)$ block-encoding with the same cost as Eqs. (46) and (47).

Similarly to the case of $P^{(3)}$, we can obtain

$$\frac{P^{(n)}(\mathbf{r}, \tau)}{I^{(n)}(\tau)} = \frac{\langle U^{(n)}(\tau) | \tilde{C}^{(n)}(\boldsymbol{\rho}) | U^{(n)}(\tau) \rangle}{\langle U^{(n)}(\tau) | \tilde{C}^{(n)}(\mathbf{0}) | U^{(n)}(\tau) \rangle} \quad (50)$$

by applying the overlap estimation algorithm [72]. To achieve error tolerance ϵ_3 , we have to make

$$\mathcal{O} \left(\frac{2^{\frac{n-2}{2}m}}{\epsilon_3} \right) \text{ queries to } \mathcal{C}^{(n)} \text{ and } O_{U^{(n)}}. \quad (51)$$

D. Taking ensemble averages

So far, we have discussed computing spatial correlations of the velocity field for a single realization of Burgers turbulence. As discussed in Sec. D.2 of Ref. [15], we can extend it to taking ensemble averages of multiple realizations.

To this end, we assume that we have $N_{\text{en}} = 2^{n_{\text{en}}}$ initial conditions and have an oracle

$$O_{\text{IC}} := \left(\sum_{\alpha=1}^{N_{\text{en}}} O_{\psi'_0(\alpha)} \otimes |\alpha\rangle \langle \alpha| \right) (1_{N_x} \otimes H^{\otimes n_{\text{en}}}) \quad (52)$$

so that a superposition of N_{en} initial conditions are generated as

$$O_{\text{IC}}|0\rangle = 2^{-\frac{n_{\text{en}}}{2}} \sum_{\alpha=1}^{N_{\text{en}}} |\partial_x \psi^{(\alpha)}(0)\rangle |\alpha\rangle, \quad (53)$$

where we introduce additional n_{en} qubits to label the ensembles.

We then integrate the heat equation as explained in Sec. III B. We apply $O_{\psi'} \otimes 1_{N_{\text{en}}}$ to the state (53) with error tolerance ϵ_1 for the integration algorithm and ϵ_2 for the block-encoding of A . With the approximation (19), this yields

$$2^{-\frac{n_{\text{en}}}{2}} \sum_{\alpha=1}^{N_{\text{en}}} |\mathbf{u}^{(\alpha)}\rangle |\alpha\rangle, \quad (54)$$

where $|\mathbf{u}^{(\alpha)}\rangle := \sum_j \frac{u_j^{(\alpha)}}{\|\mathbf{u}^{(\alpha)}\|} |j\rangle$ encodes the solution $u^{(\alpha)}$ with the α -th initial condition. By applying the coarse-graining operation described in Sec. III C 2, we obtain

$$2^{-\frac{n_{\text{en}}}{2}} \sum_{\alpha=1}^{N_{\text{en}}} |\mathbf{u}^{(\alpha)}\rangle_{\text{cg}} |\alpha\rangle, \quad (55)$$

where $|\mathbf{u}^{(\alpha)}\rangle_{\text{cg}}$ is given as Eq. (29) with $u = u^{(\alpha)}$.

Then, using the above operation, we can generate

$$|U^{(n)}\rangle_{\text{en}} := 2^{-\frac{n_{\text{en}}}{2}} \sum_{\alpha=1}^{N_{\text{en}}} |U^{(n,\alpha)}\rangle |\alpha\rangle, \quad (56)$$

where $U^{(n,\alpha)}$ is given as Eq. (44) or (48) with $u = u^{(\alpha)}$. Defining the ensemble average of the n -point function as

$$\langle P^{(n)}(\mathbf{r}) \rangle := 2^{-n_{\text{en}}} \sum_{\alpha=1}^{N_{\text{en}}} P^{(n,\alpha)}(\mathbf{r}), \quad (57)$$

where $P^{(n,\alpha)}(\mathbf{r})$ is the n -point function for $u^{(\alpha)}$, and $\langle I^{(n)} \rangle := \langle P^{(n)}(\mathbf{0}) \rangle$, we see that

$$\frac{\langle P^{(n)}(\mathbf{r}) \rangle}{\langle I^{(n)} \rangle} = \frac{\langle U^{(n)}|_{\text{en}} \tilde{C}^{(n)}(\boldsymbol{\rho}) \otimes 1_{N_{\text{en}}} |U^{(n)}\rangle_{\text{en}}}{\langle U^{(n)}|_{\text{en}} \tilde{C}^{(n)}(\mathbf{0}) \otimes 1_{N_{\text{en}}} |U^{(n)}\rangle_{\text{en}}}, \quad (58)$$

and thus we can calculate this in a parallel way to the procedure in Sec. III C. Namely, we perform the overlap estimation with an error tolerance ϵ_3 , by replacing $C^{(2)}$ and $\mathcal{C}^{(n)}$ with $C^{(2)} \otimes 1$ and $\mathcal{C}^{(n)} \otimes 1$, respectively.

IV. DISCUSSION

A. Total complexity

We first estimate the complexity of the algorithm, apart from the discretization error, which is common in both quantum and classical algorithms and may be reduced

by implementing higher-order stencils. Our algorithm accepts errors of $\mathcal{O}(\epsilon_1 + \tau\epsilon_2 + \epsilon_3 + \epsilon_4)$ for $P^{(n)}/I^{(n)}$. By taking $\tau\epsilon_2 \sim \epsilon$ and $\epsilon_1 \sim \epsilon_3 \sim \epsilon_4 \sim \epsilon$ to be of the order of the desired error tolerance ϵ , we require query complexities at each step of the operation as summarized in TABLE I. In total, to measure $P^{(n)}/I^{(n)}$ for a general n , we make

$$\begin{aligned} & \mathcal{O}\left(2^{\frac{n-2}{2}m} n \frac{\|\partial_x \psi_0\|}{\|\partial_x \psi(\tau)\|} \frac{\tau}{\epsilon} \text{polylog}\left(\frac{1}{\epsilon}\right) \left(n_x + \log^{\frac{5}{2}}\left(\frac{\tau}{\epsilon}\right)\right)\right) \\ &= \tilde{\mathcal{O}}\left(2^{\frac{n-2}{2}m} n \frac{\|\partial_x \psi_0\|}{\|\partial_x \psi(\tau)\|} \frac{n_x \tau}{\epsilon}\right) \end{aligned} \quad (59)$$

uses of sparse-access queries and other fundamental gates and use

$$\mathcal{O}\left(n_x + \log^{\frac{5}{2}}\left(\frac{\tau}{\epsilon}\right)\right) \quad (60)$$

ancilla qubits, where $n_x = \log N_x$ and $\tau = \nu t / \Delta x^2$. In particular, for $n = 2$, we can use Eq. (25) to construct $\mathcal{C}^{(n=2)}$ with $\mathcal{O}(n_x^2)$ fundamental gates instead of applying the sparse-oracle-based block-encoding technique, and the number of uses of other oracles and fundamental gates is also reduced. Note that, if $\partial\psi_0$ has large long-wavelength modes, which dissipate slowly, then the growth of the factor $\|\partial_x \psi_0\| / \|\partial_x \psi(\tau)\|$ is slow as well.

This can be significantly less than a naive estimate of the classical complexity. Since $\psi(x, t)$ is the convolution of $\psi(0, t)$ and the heat kernel, it takes $\mathcal{O}(N_x)$ computations to obtain $u(x, t)$ for a given (x, t) . To compute $P^{(n)}$, we identify the ensemble average with the spatial average and compute $u(x, t)$ at all sites x_j for a given t , which costs $\mathcal{O}(N_x^2)$ computations in total. Therefore, when one increases N_x to achieve high-resolution simulation, our quantum algorithm is exponentially faster.

B. Validity of the assumptions and generalization

Next, let us clarify what assumptions are made for our algorithm to work and discuss possible generalizations to go beyond the direct application of the algorithm.

1. Periodic boundary condition

In Sec. III A, we imposed the periodic boundary condition on ψ . We can straightforwardly generalize the algorithm to another boundary condition, say the Dirichlet boundary condition, by just modifying the matrix A and $C^{(n)}$. The complexity estimate of our algorithm does not change with this modification.

2. Approximation in Eq. (18)

An issue is the applicability of Eq. (18). The approximation is not always valid for a large Reynolds number. If

purpose	n	oracle	number of uses
initial value encoding	-	$O_{\psi'_0}$	$\mathcal{O}\left(\frac{\ \partial_x \psi_0\ }{\ \partial_x \psi(\tau)\ } \frac{2^{\frac{n-2}{2}m} n}{\epsilon}\right) = n \times \text{Eq. (15)} \times \text{Eq. (51)}$
time integration	-	sparse-access oracles for A	$\mathcal{O}\left(\frac{\ \partial_x \psi_0\ }{\ \partial_x \psi(\tau)\ } \frac{2^{\frac{n-2}{2}m} n \tau}{\epsilon} \text{polylog}\left(\frac{1}{\epsilon}\right)\right) = n \times \text{Eq. (14)} \times \text{Eq. (17)} \times \text{Eq. (51)}$
	-	other fundamental gates	$\mathcal{O}\left(\frac{\ \partial_x \psi_0\ }{\ \partial_x \psi(\tau)\ } \frac{2^{\frac{n-2}{2}m} n \tau}{\epsilon} \left(n_x + \log^{\frac{5}{2}}\left(\frac{\tau}{\epsilon}\right)\right) \text{polylog}\left(\frac{1}{\epsilon}\right)\right) = n \times \text{Eq. (14)} \times \text{Eq. (16)} \times \text{Eq. (51)}$
block-encoding of $\tilde{C}^{(n)}$	$n \geq 3$	sparse-access oracles for $\tilde{C}^{(n)}$	$\mathcal{O}\left(\frac{2^{\frac{n-2}{2}m}}{\epsilon}\right) = \text{Eq. (46)} \times \text{Eq. (51)}$
		other fundamental gates	$\mathcal{O}\left(\frac{2^{\frac{n-2}{2}m}}{\epsilon} \left(nn_x + \log^{\frac{5}{2}}\left(\frac{n!}{\epsilon}\right)\right)\right) = \text{Eq. (47)} \times \text{Eq. (51)}$
	2	fundamental gates	$\mathcal{O}\left(\frac{n_x^2}{\epsilon}\right) = \text{Eq. (27)} \times \text{Eq. (51)}$

TABLE I. The number of uses of various oracles in the proposed method to calculate the n -point function. Subdominant contributions and additional ones for controlled operations are neglected.

we decompose ψ into homogeneous and fluctuation parts as $\psi(x) = \bar{\psi} + \delta\psi(x)$, a naive estimate $\delta\psi/\bar{\psi} \sim \text{Re}$ implies that the equation is not a good approximation when the Reynolds number is large.

To classically demonstrate the difference between using the approximation Eq. (18) and the exact relation Eq. (4), we take a random initial condition,

$$\psi(x, 0) = e^{\xi_0 + \sum_{j=1}^{j_{\max}} (\xi_j \cos \frac{2\pi j x}{L} + \xi_{j_{\max}+j} \sin \frac{2\pi j x}{L})}, \quad (61)$$

where ξ_j , $j = 1, \dots, 2j_{\max}$ are random variables generated by a normal distribution with the expectation value 0 and the standard deviation σ_ξ . Here we take $\sigma_\xi = 0.3$, $j_{\max} = 5$, and $n_x = 7$, and obtain an initial condition of ψ as shown in the red-solid line in Fig. 1. The green-solid and beige-solid lines represent the evolution of ψ , and the blue-dashed line represents $\bar{\psi}$. We see that a long-wavelength mode survives and ψ typically deviates from $\bar{\psi}$ by more than $\sim 10\%$ until $\tau = 0.02$. As a test of the validity of the approximation, we plot in Fig. 2 the flatness β defined as

$$\beta := \frac{I^{(4)}}{(I^{(2)})^2} - 3. \quad (62)$$

This generally approaches $\beta = -3/2$ in a perturbative regime (see Appendix A), and we thus expect that calculating β would be useful as a test also in quantum computing on future real hardware. In Fig. 2, both the exact value (solid line) and the approximation (dashed line) converge to the asymptotic value in the perturbative regime, $\beta = -3/2$, at $\tau \sim 0.02$. We see that our approximation works in the late dissipative regime, even though $\delta\psi$ is set large at the beginning.

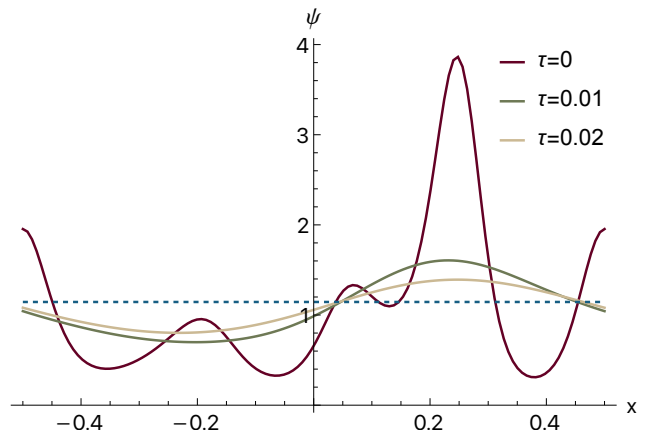


FIG. 1. An example of the evolution of ψ with a random initial condition given in Eq. (61) (Red-solid line at $\tau = 0$, green-solid at $\tau = 0.01$, and beige-solid at $\tau = 0.02$). We also show the spatial average $\bar{\psi}$ with the blue-dashed line.

3. Homogeneous background

We assumed the existence of a homogeneous background $\bar{\psi}$. Therefore, for example, a Brownian motion, which is often taken in the literature as the initial condition [74–77], is beyond the direct applicability of our algorithm because it does not have a homogeneous baseline $\bar{\psi}$.

To generalize the assumption, suppose that we can find a linear baseline for the initial condition of interest, namely, $\psi_j(0) = \bar{\psi}_j(0) + \delta\psi_j(0)$, where $\bar{\psi}_j(0) = aj + b$ and $\delta\psi_j(0)$ is statistically homogeneous. Then, the baseline does not evolve in time, and a similar discussion in the previous sections holds. We may modify definitions

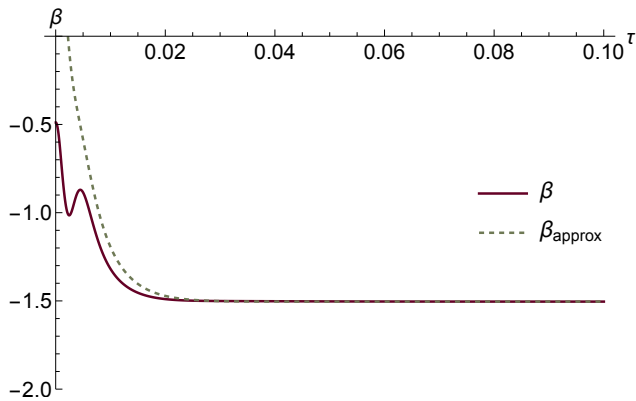


FIG. 2. Comparison between the values of flatness β obtained by the approximation Eq. (18) (green-dashed) and the exact relation Eq. (4) (red-solid).

of $C_j^{(n)}$ and replace $C_j^{(n)}/(\bar{\psi})^n$ with

$$\frac{1}{(\bar{\psi})^n} C_j^{(n)} \rightarrow \sum_{\sigma} \delta_{j-\sigma} \frac{c_{\sigma}^{(n)}}{(a(j_1 - \sigma_1) + b)^2}. \quad (63)$$

However, we note that how large the computational cost becomes depends on $\min\{ax + b\}$ because it affects the cost of block-encoding and the error tolerance in the measurement. We will leave such an extension for future work.

V. CONCLUSION

We developed an FTQC algorithm to measure the statistical properties of Burgers turbulence. By applying the Cole–Hopf transformation, we are able to effectively linearize the non-linear equation in terms of a redefined field. From the solution as a quantum state, we can extract classical information about the multi-point functions of the original velocity field. Although there is a limitation in the information extraction step for turbulence with a high Reynolds number, our algorithm offers exponential advantages over classical methods in terms of the number of spatial grids N_x (from $\mathcal{O}(N_x^2)$ to $\tilde{\mathcal{O}}(\text{polylog} N_x)$). This work serves as a proof of concept for solving non-linear systems using quantum computing.

ACKNOWLEDGEMENT

The work of FU is supported by JSPS KAKENHI Grant No. JP23KJ0642. The work of KM is supported by MEXT Quantum Leap Flagship Program (MEXT Q-LEAP) Grant no. JPMXS0120319794, JSPS KAKENHI Grant No. JP22K11924, and JST COI-NEXT Program Grant No. JPMJPF2014. The work of KF is supported by JSPS KAKENHI Grant No. JP20K14512.

Appendix A: Perturbative flatness for a plane wave initial condition

For the plane-wave initial condition,

$$\psi(x, 0) = 1 + \delta_m \sin\left(\frac{2\pi m x}{L}\right), \quad m \in \mathbb{Z}_+, \quad (A1)$$

one can analytically integrate Eq. (5) to obtain

$$\psi(x, t) = 1 + \delta_m \sin\left(\frac{2\pi m x}{L}\right) \exp\left(-\frac{4\pi^2 m^2 \tau}{N_x^2}\right). \quad (A2)$$

In the large τ limit, it is clear that $\|\psi_0\|/\|\psi(\tau)\| = 1$.

We can also easily compute β . The velocity field, u , is computed by the relation (4), and by expanding $\langle u^2 \rangle$ and $\langle u^4 \rangle$ by powers of δ_m , one obtains

$$\begin{aligned} \langle u^2 \rangle &= \left(\frac{4\pi m \nu \delta_m}{L}\right)^2 \frac{1}{2} \exp\left(-\frac{8\pi^2 m^2 \tau}{N_x^2}\right) \\ &\quad \cdot \left(1 + \frac{3\delta_m^2}{4} \exp\left(-\frac{8\pi^2 m^2 \tau}{N_x^2}\right) + \dots\right), \quad (A3) \end{aligned}$$

$$\begin{aligned} \langle u^4 \rangle &= \left(\frac{4\pi m \nu \delta_m}{L}\right)^4 \frac{3}{8} \exp\left(-\frac{16\pi^2 m^2 \tau}{N_x^2}\right) \\ &\quad \cdot \left(1 + \frac{5\delta_m^2}{3} \exp\left(-\frac{8\pi^2 m^2 \tau}{N_x^2}\right) + \dots\right). \quad (A4) \end{aligned}$$

By substituting it into Eq. (62), one obtains

$$\beta = -\frac{3}{2} \left(1 - \frac{\delta_m^2}{6} \exp\left(-\frac{8\pi^2 m^2 \tau}{N_x^2}\right) + \dots\right). \quad (A5)$$

-
- [1] S. P. Jordan, K. S. M. Lee, and J. Preskill, Quantum Algorithms for Quantum Field Theories, *Science* **336**, 1130 (2012), [arXiv:1111.3633 \[quant-ph\]](#).
[2] S. P. Jordan, K. S. M. Lee, and J. Preskill, Quantum Computation of Scattering in Scalar Quantum Field Theories, *Quant. Inf. Comput.* **14**, 1014 (2014), [arXiv:1112.4833 \[hep-th\]](#).
[3] S. P. Jordan, K. S. M. Lee, and J. Preskill, Quantum Al-

- gorithms for Fermionic Quantum Field Theories, (2014), [arXiv:1404.7115 \[hep-th\]](#).
[4] S. P. Jordan, H. Krovi, K. S. M. Lee, and J. Preskill, BQP-completeness of Scattering in Scalar Quantum Field Theory, *Quantum* **2**, 44 (2018), [arXiv:1703.00454 \[quant-ph\]](#).
[5] J. Preskill, Simulating quantum field theory with a quantum computer, *PoS LATTICE2018*, 024 (2018),

- arXiv:1811.10085 [hep-lat].
- [6] C. W. Bauer et al., Quantum Simulation for High-Energy Physics, *PRX Quantum* **4**, 027001 (2023), arXiv:2204.03381 [quant-ph].
- [7] A. Di Meglio et al., Quantum Computing for High-Energy Physics: State of the Art and Challenges. Summary of the QC4HEP Working Group, (2023), arXiv:2307.03236 [quant-ph].
- [8] A. Delgado et al., Quantum Computing for Data Analysis in High-Energy Physics, in *Snowmass 2021* (2022) arXiv:2203.08805 [physics.data-an].
- [9] A. Kaufman, D. Sundry, and M. McGuigan, Quantum computation for early universe cosmology in *2019 New York Scientific Data Summit: Data-Driven Discovery in Science and Industry* (2019).
- [10] J. Liu and Y.-Z. Li, On Quantum Simulation Of Cosmic Inflation, *Phys. Rev. D* **104**, 086013 (2021), arXiv:2009.10921 [quant-ph].
- [11] A. Joseph, J.-P. Varela, M. P. Watts, T. White, Y. Feng, M. Hassan, and M. McGuigan, Quantum Computing for Inflationary, Dark Energy and Dark Matter Cosmology, (2021), arXiv:2105.13849 [quant-ph].
- [12] G. Czelusta and J. Mielczarek, Quantum variational solving of the Wheeler-DeWitt equation, *Phys. Rev. D* **105**, 126005 (2022), arXiv:2111.03038 [gr-qc].
- [13] P. Mocz and A. Szasz, Towards Cosmological Simulations of Dark Matter on Quantum Computers, *Astrophys. J.* **910**, 29 (2021), arXiv:2101.05821 [astro-ph.CO].
- [14] S. Yamazaki, F. Uchida, K. Fujisawa, K. Miyamoto, and N. Yoshida, Quantum algorithm for collisionless Boltzmann simulation of self-gravitating systems, *Computers and Fluids* (2025), arXiv:2303.16490 [quant-ph].
- [15] K. Miyamoto, S. Yamazaki, F. Uchida, K. Fujisawa, and N. Yoshida, Quantum algorithm for the Vlasov simulation of the large-scale structure formation with massive neutrinos, *Phys. Rev. Res.* **6**, 013200 (2024), arXiv:2310.01832 [quant-ph].
- [16] H. Higuchi, J. W. Pedersen, K. Toyoizumi, K. Yoshikawa, C. Kiumi, and A. Yoshikawa, Quantum Calculation for Two-Stream Instability and Advection Test of Vlasov-Maxwell Equations: Numerical Evaluation of Hamiltonian Simulation, (2024), arXiv:2408.11550 [physics.plasm-ph].
- [17] J. Preskill, Quantum Computing in the NISQ era and beyond, *Quantum* **2**, 79 (2018), arXiv:1801.00862 [quant-ph].
- [18] P. W. Shor, Fault-tolerant quantum computation (1996) arXiv:quant-ph/9605011.
- [19] E. T. Campbell, B. M. Terhal, and C. Vuillot, Roads towards fault-tolerant universal quantum computation, *Nature* **549**, 172 (2017).
- [20] P. Webster, M. Vasmer, T. R. Scruby, and S. D. Bartlett, Universal fault-tolerant quantum computing with stabilizer codes, *Phys. Rev. Res.* **4**, 013092 (2022), arXiv:2012.05260 [quant-ph].
- [21] R. Acharya et al. (Google Quantum AI), Suppressing quantum errors by scaling a surface code logical qubit, *Nature* **614**, 676 (2023), arXiv:2207.06431 [quant-ph].
- [22] B. N. Todorova and R. Steijl, Quantum algorithm for the collisionless Boltzmann equation, *Journal of Computational Physics* **409**, 109347 (2020).
- [23] M. Henon, Vlasov equation, *Astronomy & Astrophysics* **114**, 211 (1982).
- [24] A. W. Harrow, A. Hassidim, and S. Lloyd, Quantum Algorithm for Linear Systems of Equations, *Phys. Rev. Lett.* **103**, 150502 (2009), arXiv:0811.3171 [quant-ph].
- [25] B. D. Clader, B. C. Jacobs, and C. R. Sprouse, Preconditioned Quantum Linear System Algorithm, *Phys. Rev. Lett.* **110**, 250504 (2013).
- [26] D. W. Berry, High-order quantum algorithm for solving linear differential equations, *J. Phys. A* **47**, 105301 (2014).
- [27] C. Andrew M., K. Robin, and S. Rolando D., Quantum Algorithm for Systems of Linear Equations with Exponentially Improved Dependence on Precision, *SIAM J. Comput.* **46**, 1920 (2017), arXiv:1511.02306 [quant-ph].
- [28] P. C. S. Costa, S. Jordan, and A. Ostrander, Quantum algorithm for simulating the wave equation, *Phys. Rev. A* **99**, 012323 (2019).
- [29] Y. Sato, H. Tezuka, R. Kondo, and N. Yamamoto, Quantum algorithm for partial differential equations of non-conservative systems with spatially varying parameters, (2024), arXiv:2407.05019 [quant-ph].
- [30] L. D. Landau and E. M. Lifshitz, *Fluid Mechanics* (1987).
- [31] A. Roper Pol, S. Mandal, A. Brandenburg, T. Kahniashvili, and A. Kosowsky, Numerical simulations of gravitational waves from early-universe turbulence, *Phys. Rev. D* **102**, 083512 (2020), arXiv:1903.08585 [astro-ph.CO].
- [32] A. Brandenburg, E. Clarke, T. Kahniashvili, A. J. Long, and G. Sun, Relic gravitational waves from the chiral plasma instability in the standard cosmological model, *Phys. Rev. D* **109**, 043534 (2024), arXiv:2307.09385 [astro-ph.CO].
- [33] R. Sharma and A. Brandenburg, Low frequency tail of gravitational wave spectra from hydromagnetic turbulence, *Phys. Rev. D* **106**, 103536 (2022), arXiv:2206.00055 [astro-ph.CO].
- [34] A. Brandenburg, K. Enqvist, and P. Olesen, Large scale magnetic fields from hydromagnetic turbulence in the very early universe, *Phys. Rev. D* **54**, 1291 (1996), arXiv:astro-ph/9602031.
- [35] R. Banerjee and K. Jedamzik, The Evolution of cosmic magnetic fields: From the very early universe, to recombination, to the present, *Phys. Rev. D* **70**, 123003 (2004), arXiv:astro-ph/0410032.
- [36] T. Kahniashvili, A. G. Tevzadze, A. Brandenburg, and A. Neronov, Evolution of Primordial Magnetic Fields from Phase Transitions, *Phys. Rev. D* **87**, 083007 (2013), arXiv:1212.0596 [astro-ph.CO].
- [37] A. Brandenburg, T. Kahniashvili, S. Mandal, A. Roper Pol, A. G. Tevzadze, and T. Vachaspati, Evolution of hydromagnetic turbulence from the electroweak phase transition, *Phys. Rev. D* **96**, 123528 (2017), arXiv:1711.03804 [astro-ph.CO].
- [38] F. Uchida, M. Fujiwara, K. Kamada, and J. Yokoyama, New comprehensive description of the scaling evolution of the cosmological magneto-hydrodynamic system, (2024), arXiv:2405.06194 [astro-ph.CO].
- [39] G. I. Ogilvie, Lecture notes: Astrophysical fluid dynamics, arXiv e-prints, arXiv:1604.03835 (2016), arXiv:1604.03835 [astro-ph.SR].
- [40] S. K. Leyton and T. J. Osborne, A quantum algorithm to solve nonlinear differential equations, arXiv e-prints, arXiv:0812.4423 (2008), arXiv:0812.4423 [quant-ph].
- [41] F. Gaitan, Finding flows of a Navier-Stokes fluid through quantum computing, *npj Quantum Information* **6**, 61 (2020).
- [42] Z. Meng and Y. Yang, Quantum computing of fluid

- dynamics using the hydrodynamic Schrödinger equation, *Phys. Rev. Res.* **5**, 033182 (2023), [arXiv:2302.09741 \[physics.flu-dyn\]](#).
- [43] F. Oz, R. K. S. S. Vuppala, K. Kara, and F. Gaitan, Solving Burgers' equation with quantum computing, *Quant. Inf. Proc.* **21**, 30 (2022).
- [44] N. Ray, T. Banerjee, B. Nadiga, and S. Karra, Towards Solving the Navier-Stokes Equation on Quantum Computers, [arXiv e-prints](#), [arXiv:1904.09033 \(2019\)](#), [arXiv:1904.09033 \[cs.NA\]](#).
- [45] M. Syamlal, C. Copen, M. Takahashi, and B. Hall, Computational Fluid Dynamics on Quantum Computers, [arXiv e-prints](#), [arXiv:2406.18749 \(2024\)](#), [arXiv:2406.18749 \[quant-ph\]](#).
- [46] J.-P. Liu, H. Ø. Kolden, H. K. Krovi, N. F. Loureiro, K. Trivisa, and A. M. Childs, Efficient quantum algorithm for dissipative nonlinear differential equations, *Proceedings of the National Academy of Science* **118**, e2026805118 (2021), [arXiv:2011.03185 \[quant-ph\]](#).
- [47] A. Engel, G. Smith, and S. E. Parker, Linear embedding of nonlinear dynamical systems and prospects for efficient quantum algorithms, *Physics of Plasmas* **28**, 062305 (2021), [arXiv:2012.06681 \[physics.plasm-ph\]](#).
- [48] H. Krovi, Improved quantum algorithms for linear and nonlinear differential equations, *Quantum* **7**, 913 (2023), [arXiv:2202.01054 \[quant-ph\]](#).
- [49] H. Bateman, Some Recent Researches on the Motion of Fluids, *Monthly Weather Review* **43**, 163 (1915).
- [50] J. M. Burgers, A mathematical model illustrating the theory of turbulence, *Advances in applied mechanics* **1**, 171 (1948).
- [51] K. Ohkitani and M. Dowker, Numerical study on comparison of Navier-Stokes and Burgers equations, *Physics of Fluids* **24**, 055113-055113-20 (2012).
- [52] K. Ohkitani, Generalized incompressible fluid dynamical system interpolating between the Navier-Stokes and Burgers equations in two dimensions, [arXiv e-prints](#), [arXiv:2408.06529 \(2024\)](#), [arXiv:2408.06529 \[physics.flu-dyn\]](#).
- [53] E. Hopf, The partial differential equation $u_t + uu_x = \mu_{xx}$, *Communications on Pure and Applied mathematics* **3**, 201 (1950).
- [54] J. D. Cole, On a quasi-linear parabolic equation occurring in aerodynamics, *Quarterly of applied mathematics* **9**, 225 (1951).
- [55] D. T. Jeng, R. Foerster, S. Haaland, and W. C. Meecham, Statistical Initial-Value Problem for Burgers' Model Equation of Turbulence, *Physics of Fluids* **9**, 2114 (1966).
- [56] T. Gotoh and R. H. Kraichnan, Statistics of decaying Burgers turbulence, *Physics of Fluids A* **5**, 445 (1993).
- [57] R. Ryan, The Statistics of Burgers Turbulence Initialized with Fractional Brownian Noise Data, *Communications in Mathematical Physics* **191**, 71 (1998).
- [58] T. Gotoh, Probability density functions in steady-state Burgers turbulence, *Physics of Fluids* **11**, 2143 (1999).
- [59] S. Alam, P. K. Sahu, and M. K. Verma, Universal functions for Burgers turbulence, *Physical Review Fluids* **7**, 074605 (2022).
- [60] J. Bec and K. Khanin, Burgers turbulence, *Physics Reports* **447**, 1 (2007), [arXiv:0704.1611 \[nlin.CD\]](#).
- [61] D. An, A. M. Childs, and L. Lin, Quantum algorithm for linear non-unitary dynamics with near-optimal dependence on all parameters, (2023), [arXiv:2312.03916 \[quant-ph\]](#).
- [62] N. Linden, A. Montanaro, and C. Shao, Quantum vs. Classical Algorithms for Solving the Heat Equation, *Communications in Mathematical Physics* **395**, 601 (2022).
- [63] L. Grover and T. Rudolph, Creating superpositions that correspond to efficiently integrable probability distributions, [arXiv e-prints](#) (2002), [arXiv:quant-ph/0208112 \[quant-ph\]](#).
- [64] Y. R. Sanders, G. H. Low, A. Scherer, and D. W. Berry, Black-box quantum state preparation without arithmetic, *Phys. Rev. Lett.* **122**, 020502 (2019).
- [65] A. G. Rattew and B. Koczor, Preparing Arbitrary Continuous Functions in Quantum Registers With Logarithmic Complexity, [arXiv e-prints](#) (2022), [arXiv:2205.00519 \[quant-ph\]](#).
- [66] S. McArdle, A. Gilyén, and M. Berta, Quantum state preparation without coherent arithmetic, [arXiv e-prints](#) (2022), [arXiv:2210.14892 \[quant-ph\]](#).
- [67] G. Marin-Sanchez, J. Gonzalez-Conde, and M. Sanz, Quantum algorithms for approximate function loading, *Phys. Rev. Res.* **5**, 033114 (2023).
- [68] M. Moosa, T. W. Watts, Y. Chen, A. Sarma, and P. L. McMahon, Linear-depth quantum circuits for loading fourier approximations of arbitrary functions, *Quantum Science and Technology* **9**, 015002 (2023).
- [69] V. Giovannetti, S. Lloyd, and L. Maccone, Quantum Random Access Memory, *Phys. Rev. Lett.* **100**, 160501 (2008), [arXiv:0708.1879 \[quant-ph\]](#).
- [70] I. Kerenidis and A. Prakash, Quantum gradient descent for linear systems and least squares, *Phys. Rev. A* **101**, 022316 (2020).
- [71] A. Gilyén, Y. Su, G. H. Low, and N. Wiebe, Quantum singular value transformation and beyond: exponential improvements for quantum matrix arithmetics in *Proceedings of the 51st Annual ACM SIGACT Symposium on Theory of Computing* (2019) pp. 193–204, full version: [arXiv:1806.01838](#).
- [72] E. Knill, G. Ortiz, and R. D. Somma, Optimal quantum measurements of expectation values of observables, *Phys. Rev. A* **75**, 012328 (2007), [arXiv:quant-ph/0607019 \[quant-ph\]](#).
- [73] X. Li, G. Yang, C. M. Torres Jr, D. Zheng, and K. L. Wang, A class of efficient quantum incrementer gates for quantum circuit synthesis, *International Journal of Modern Physics B* **28**, 1350191 (2014).
- [74] Z.-S. She, E. Aurell, and U. Frisch, The inviscid Burgers equation with initial data of Brownian type, *Communications in Mathematical Physics* **148**, 623 (1992).
- [75] Y. G. Sinai, Statistics of shocks in solutions of inviscid Burgers equation, *Communications in Mathematical Physics* **148**, 601 (1992).
- [76] J. Bertoin, The Inviscid Burgers Equation with Brownian Initial Velocity, *Communications in Mathematical Physics* **193**, 397 (1998).
- [77] P. Valageas, Statistical Properties of the Burgers Equation with Brownian Initial Velocity, *Journal of Statistical Physics* **134**, 589 (2009), [arXiv:0810.4332 \[cond-mat.stat-mech\]](#).